

Synthesis and Evaluation of (Pyridylmethylene)tetrahydronaphthalenes/-indanes and Structurally Modified Derivatives: Potent and Selective Inhibitors of Aldosterone Synthase

Sarah Ulmschneider,[†] Ursula Müller-Vieira,[†] Christian D. Klein,[†] Iris Antes,[‡] Thomas Lengauer,[‡] and Rolf W. Hartmann^{*,†}

FR 8.2 Pharmaceutical and Medicinal Chemistry, Saarland University, P.O. Box 15 11 50, D-66041 Saarbrücken, Germany, and Max Planck Institute for Informatics, Stuhlsatzenhausweg 85, D-66123 Saarbrücken, Germany

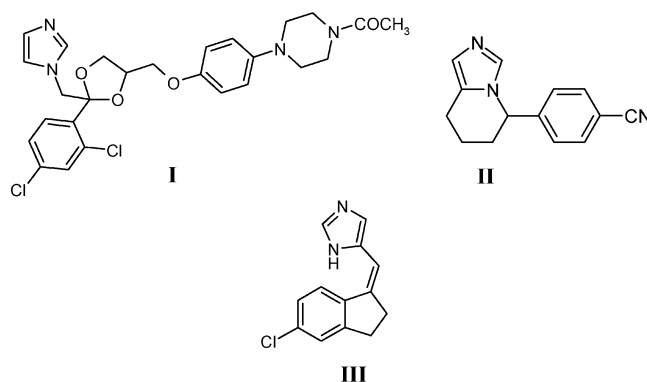
Received September 17, 2004

Elevated aldosterone levels are key effectors for the development and progression of congestive heart failure and myocardial fibrosis. Recently, we proposed inhibition of aldosterone synthase (CYP11B2) as an innovative strategy for the treatment of these diseases. In this study, the synthesis and biological evaluation of *E*- and *Z*-(pyridylmethylene)tetrahydronaphthalenes and -indanes (**1a,b**–**38a**) is described. The activity of the compounds was determined using human CYP11B2, and the selectivity was evaluated toward the human steroidogenic enzymes CYP11B1, CYP19, and CYP17. The biological results revealed a few rather selective inhibitors of CYP11B1, some compounds inhibiting both CYP11B1 and CYP11B2, and a large number of highly selective inhibitors of CYP11B2. The most active inhibitor was the 3-pyridyl compound **5a** (IC₅₀ = 7 nM). The pyrimidyl-substituted derivative **28a** was found to be the most selective CYP11B2 inhibitor (IC₅₀ = 27 nM) in this series, showing a 120-fold selectivity for CYP11B1 (IC₅₀ = 3179 nM). Molecular modeling, i.e., examination of the electronic and steric features of selected compounds and homology modeling and docking, was used to understand the structure–activity/–selectivity relationships.

Introduction

Aldosterone synthase (CYP11B2) is the key enzyme of mineralocorticoid biosynthesis. It catalyzes the conversion of 11-deoxycorticosterone to the most potent mineralocorticoid, aldosterone.¹ The adrenal aldosterone synthesis is regulated by several physiological parameters, such as the renin–angiotensin–aldosterone system (RAAS), and the plasma potassium concentration. Elevations in plasma aldosterone levels increase blood pressure and play an important role in the pathophysiology of myocardial fibrosis and congestive heart failure.² In two recent clinical studies (RALES and EPHE-SUS), the aldosterone receptor antagonists spironolactone and eplerenone were found to reduce mortality in patients with chronic congestive heart failure and in patients after myocardial infarction, respectively.^{3,4} For spironolactone, progestational and antiandrogenic side effects were observed, which are supposedly due to its steroidal structure.^{4–6} A new pharmacological approach for the treatment of hyperaldosteronism, congestive heart failure, and myocardial fibrosis was recently suggested by us: inhibition of aldosterone formation with nonsteroidal, selective CYP11B2 inhibitors.^{7,8} This strategy has two main advantages in comparison to the receptor blockade. The inhibitors can be expected to have fewer side effects than the steroidal antagonists on the endocrine system,^{7,8} since no inhibitor of a steroidogenic CYP enzyme is known to have affinity for a steroid receptor. Furthermore, it should be clinically

Chart 1. Chemical Structures of Ketoconazole (I), Fadrozole (II), and 5-[(*Z*)-(5-Chloro-2,3-dihydro-1*H*-inden-1-ylidene)methyl]-1*H*-imidazole (III)

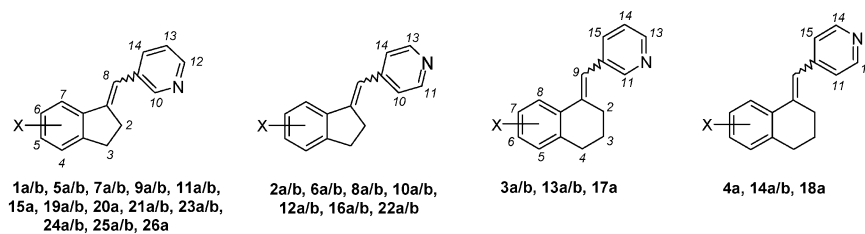


advantageous to reduce aldosterone formation rather than leaving the pathologically elevated aldosterone levels unaffected and interfering one step later at the receptor level. However, for the steroidogenic CYP targets, selectivity of inhibition is an obstacle to be overcome. For CYP19 it has been demonstrated that a selective inhibition is possible, and novel inhibitors of this enzyme are first line therapeutics for breast cancer.⁹ This goal, however, is much more difficult to achieve for CYP11B2, since the enzyme responsible for glucocorticoid biosynthesis (CYP11B1, steroid 11 β -hydroxylase) has a sequence homology of more than 93% compared to CYP11B2,^{1,10} whereas the homology of CYP19 to other steroidogenic CYPs is less than 30%.¹¹ Recently, we found the CYP19 inhibitor fadrozole (Chart 1) to be a highly potent but moderately selective inhibitor for CYP11B2 in vitro (IC₅₀ CYP11B2 = 1 nM, IC₅₀ CYP11B1 = 10 nM, IC₅₀ CYP19 = 30 nM).¹² It has

* To whom correspondence should be addressed. Phone: + 49 681 302 3424. Fax: + 49 681 302 4386. E-mail: rwh@mx.uni-saarland.de. Homepage: <http://www.uni-saarland.de/fak8/hartmann/index.htm>.

[†] Saarland University.

[‡] Max Planck Institute for Informatics.

Chart 2. Title Compounds

no	X	Isomer	no	X	Isomer	no	X	Isomer
1a	H	<i>E</i>	9b	5-Br	<i>Z</i>	19a	5-OEt	<i>E</i>
1b	H	<i>Z</i>	10a	5-Br	<i>E</i>	19b	5-OEt	<i>Z</i>
2a	H	<i>E</i>	10b	5-Br	<i>Z</i>	20a	5-OBn	<i>E</i>
2b	H	<i>Z</i>	11a	5-OMe	<i>E</i>	21a	6-Me	<i>E</i>
3a	H	<i>E</i>	11b	5-OMe	<i>Z</i>	21b	6-Me	<i>Z</i>
3b	H	<i>Z</i>	12a	5-OMe	<i>E</i>	22a	6-Me	<i>E</i>
4a	H	<i>E</i>	12b	5-OMe	<i>Z</i>	22b	6-Me	<i>Z</i>
5a	5-F	<i>E</i>	13a	6-OMe	<i>E</i>	23a	4-Me	<i>E</i>
5b	5-F	<i>Z</i>	13b	6-OMe	<i>Z</i>	23b	4-Me	<i>Z</i>
6a	5-F	<i>E</i>	14a	6-OMe	<i>E</i>	24a	4-F	<i>E</i>
6b	5-F	<i>Z</i>	14b	6-OMe	<i>Z</i>	24b	4-F	<i>Z</i>
7a	5-Cl	<i>E</i>	15a	6-OMe	<i>E</i>	25a	4-Cl	<i>E</i>
7b	5-Cl	<i>Z</i>	16a	6-OMe	<i>E</i>	25b	4-Cl	<i>Z</i>
8a	5-Cl	<i>E</i>	16b	6-OMe	<i>Z</i>	26a	7-OMe	<i>E</i>
8b	5-Cl	<i>Z</i>	17a	6,7-diOMe	<i>E</i>			
9a	5-Br	<i>E</i>	18a	6,7-diOMe	<i>E</i>			

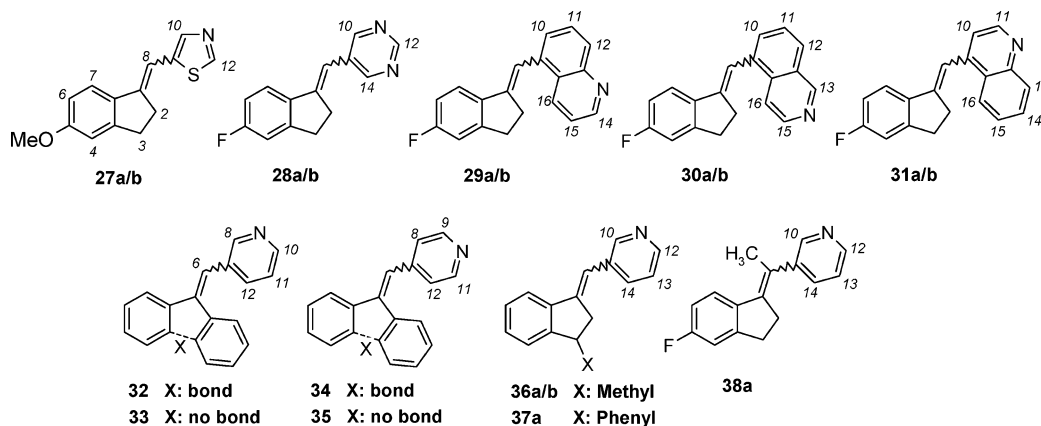
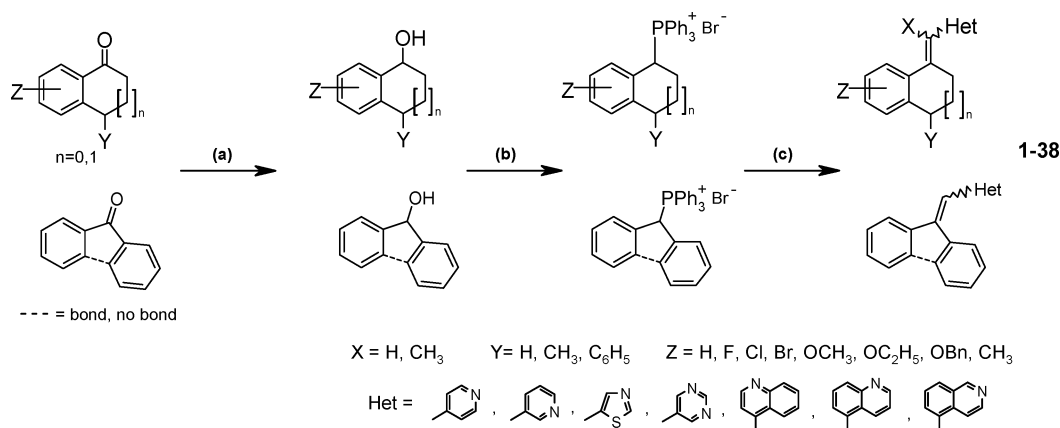
been known for sometime to lower aldosterone and cortisol levels in patients after application of a dose 10-fold higher than the therapeutical dose.^{13,14} This encouraged us to search for highly active and selective inhibitors. By testing a series of (imidazolylmethylene)-tetrahydronaphthalene and -indane derivatives we discovered potent and moderately selective inhibitors for CYP11B1, as well as for CYP11B2 and inhibitors being equally potent toward both enzymes. This series of compounds showed a slightly better selectivity profile toward CYP19 compared to fadrozole. The most active derivative was the chloro-substituted indane compound **III** (IC_{50} CYP11B2 = 4 nM, IC_{50} CYP11B1 = 20 nM, IC_{50} CYP19 = 39 nM; Chart 1).¹² Moderately potent inhibitors were discovered by screening azole-type fungicides on V79 Mzh cells (hamster fibroblasts) expressing either CYP11B1 or CYP11B2, the most active of which was ketoconazole (Chart 1),¹⁵ an unspecific inhibitor of many CYP enzymes.^{16,17}

For all of the few CYP11B2 inhibitors described so far, the selectivity toward one or more other CYP enzymes was insufficient. In the present paper, we describe modifications of compound **III** to enhance potency and selectivity and to explore the cavity in the active site of the enzyme. In the following paragraphs, the synthesis of a series of *E*- and *Z*-(pyridylmethylene)-tetrahydronaphthalenes and -indanes and compounds derived from these is described (Charts 2 and 3) as well as the determination of their biological activity regarding inhibition of human CYP11B2 for potency, and human CYP11B1, human CYP17, and CYP19 for selectivity. Molecular modeling studies were used to understand the structure–activity and structure–selectivity relationships.

Chemistry

The key step of the synthetic pathway was a Wittig reaction using heterocyclic aldehydes and phosphonium

Chart 3. Structural Modifications of the Title Compounds

Scheme 1^a

^a Conditions: (a) NaBH₄, MeOH/THF, 15 min at 0 °C, 1 h at room temperature; (b) PPh₃·HBr, benzene, 12 h, reflux; (c) heterocyclic carbaldehyde, K₂CO₃, 18-crown-6, CH₂Cl₂, 12 h, reflux.

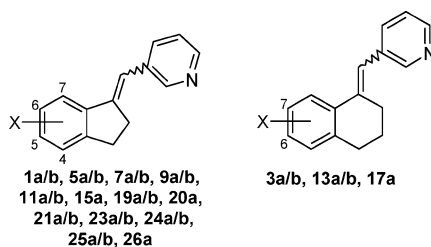
salts of the bicyclic components. Starting from the corresponding ketones, which were reduced with NaBH₄ to the alcohol intermediates,¹⁸ the obtained indanol and tetrahydronaphthol derivatives were transformed into the phosphonium salts using PPh₃·HBr prepared according to Hercouet and Le Corre¹⁹ in benzene.²⁰ Subsequently, a modified Wittig reaction followed, using K₂CO₃ as base and 18-crown-6 as phase-transfer catalyst (Scheme 1).

Most of the ketones and heterocyclic aldehydes were commercially available. 5-Ethoxyindan-1-one and 5-(benzyloxy)indan-1-one were synthesized by a nucleophilic substitution of ethyl bromide or benzyl bromide, respectively, with 5-hydroxyindan-1-one using sodium ethanolate in ethanol.²¹ 6-Methylindan-1-one and 7-methoxyindan-1-one were prepared by cyclization of the substituted phenylpropionic acids with polyphosphoric acid.²² For the preparation of the 4-substituted indanones, 3-(2-fluorophenyl)propanoic acid was synthesized in two steps as starting material: Knoevenagel reaction of malonic acid and 2-fluorobenzaldehyde,²³ followed by catalytic reduction of the generated 3-(2-fluorophenyl) acrylic acid with H₂/PtO₂·H₂O.²⁴ The fluorinated phenylpropanoic acid and the commercially available 3-(2-chlorophenyl)propanoic acid were transformed into the acid chlorides 3-(2-fluorophenyl)propanoyl chloride and 3-(2-chlorophenyl)propanoyl chloride and subsequently cyclized with AlCl₃ as described by Musso et al.²⁴ to get 4-fluoroindan-1-one and 4-chloro-

indan-1-one. 1,3-Thiazole-5-carbaldehyde was prepared in three steps as described by Dondoni et al.²⁵ lithiation of 2-trimethylsilylthiazole, subsequent quenching with *N*-formylmorpholine, and hydrolysis with HCl in dry diethyl ether. Pyrimidine-5-carbaldehyde was synthesized according to Rho et al. with slight modifications:²⁶ the bromo-lithium exchange of 5-bromopyrimidine was accomplished with *tert*-butyllithium; quenching with ethyl formiate and hydrolysis with HCl gave the heterocyclic aldehyde. After the Wittig reaction, a mixture of *E*- and *Z*-isomers was obtained in moderate to good yields (10–90%), which could be easily separated by flash column chromatography. The isomers were subsequently transformed into stable hydrochlorides (in some cases oxalates) and could be distinguished by NMR as we recently described for the (imidazolylmethylene)-tetrahydronaphthalenes and -indanes.¹² As an example, see NMR data from compounds **1a,b**–**3a,b** in the Experimental Section.

Biological Results

Inhibition of Human Adrenal Corticoids Producing CYP11B1 and CYP11B2 In Vitro (Tables 1–3). The inhibitory activities of the compounds were determined using our screening system.⁷ Human CYP11B2 expressed in fission yeast was incubated with [¹⁴C]deoxycorticosterone as substrate in the presence of the inhibitor at a concentration of 500 nM. The product

Table 1. (3-Pyridylmethylene)tetrahydronaphthalenes and -indanes: Inhibition of Human Adrenal CYP11B1 and CYP11B2, Human CYP17, and Human CYP19 in Vitro

compd	X	isomer	% inhibition		IC ₅₀ (nM)		human CYP19 ^{h,i}	selectivity factor ^j
			human hCYP11B2 ^{a,b}	human CYP17 ^{c,d}	V79 11B1 hCYP11B1 ^{e,f}	V79 11B2 hCYP11B2 ^{e,g}		
1a	H	<i>E</i>	82	14	888	11	2040	80.7
1b	H	<i>Z</i>	83	33	87	92	3550	0.9
3a	H	<i>E</i>	70	9	715	22	6580	32.5
3b	H	<i>Z</i>	68	24	1424	141	3790	10.1
5a	5-F	<i>E</i>	88	17	311	7	2540	44.4
5b	5-F	<i>Z</i>	89	16	125	11	2490	11.4
7a	5-Cl	<i>E</i>	75	26	1472	26	4260	56.6
7b	5-Cl	<i>Z</i>	68	28	270	73	4050	3.7
9a	5-Br	<i>E</i>	60	16	1937	37	7830	52.4
9b	5-Br	<i>Z</i>	58	24	320	171	7370	1.9
11a	5-OMe	<i>E</i>	79	36	1448	34	4310	42.6
11b	5-OMe	<i>Z</i>	81	49	790	26	5570	30.4
13a	6-OMe	<i>E</i>	52	20	903	57	1130	15.8
13b	6-OMe	<i>Z</i>	53	17	206	878	4000	0.2
15a	6-OMe	<i>E</i>	29	5	nd	nd	6360	—
17a	6,7-di-OMe	<i>E</i>	5	6	nd	nd	980	—
19a	5-OEt	<i>E</i>	67	13	2368	79	7080	30.0
19b	5-OEt	<i>Z</i>	52	6	2697	248	7680	10.9
20a	5-OBn	<i>E</i>	0	1	nd	nd	>36000	—
21a	6-Me	<i>E</i>	27	3	nd	nd	3930	—
21b	6-Me	<i>Z</i>	43	2	nd	nd	4600	—
23a	4-Me	<i>E</i>	52	40	763	108	4720	7.1
23b	4-Me	<i>Z</i>	12	16	nd	nd	12630	—
24a	4-F	<i>E</i>	84	42	774	21	1810	36.9
24b	4-F	<i>Z</i>	40	53	nd	nd	180	—
25a	4-Cl	<i>E</i>	92	14	304	9	130	33.8
25b	4-Cl	<i>Z</i>	83	32	657	31	230	21.1
26a	7-OMe	<i>E</i>	76	5	955	27	9740	35.4
ketoconazole	—	—	36	40	224	81	nd	2.8
fadrozole	—	—	68	5	10	1	30	10

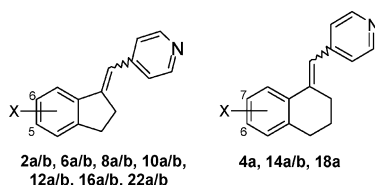
^a Mean value of four determinations, standard deviation less than 10%. ^b *S. pombe* expressing human CYP11B2; substrate deoxycorticosterone, 100 nM; inhibitor, 500 nM. ^c Mean value of four determinations, standard deviation less than 10%. ^d *E. coli* expressing human CYP17; 5 mg/mL of protein; substrate progesterone, 2.5 μM; inhibitor, 2.5 μM. ^e Mean value of four determinations, standard deviation less than 20%. nd = not determined. ^f Hamster fibroblasts expressing human CYP11B1; substrate deoxycorticosterone, 100 nM. ^g Hamster fibroblasts expressing human CYP11B2; substrate deoxycorticosterone, 100 nM. ^h Mean value of four determinations, standard deviation less than 5%. nd = not determined. ⁱ Human placental CYP19; 1 mg/mL of protein; substrate androstenedione, 500 nM. ^j IC₅₀ CYP11B1/IC₅₀ CYP11B2.

formation was monitored by HPTLC using a phosphoimager system.

Most of the 3-pyridyl-substituted derivatives (Table 1) showed a pronounced inhibitory activity similar to or higher than the reference fadrozole (68%). The 6-methylated and the 4-fluorinated compound **21b** and **24b** had moderate activity (≈40%), while compounds **17a**, **20a**, **21a**, and **23b** showed little or no activity (<30%). With the exception of the 6-methylated isomers **21a,b**, the *E*-isomers showed a similar or slightly higher inhibition than the corresponding *Z*-isomers. Ring contraction from tetraline to indane enhanced the activity. Introduction of halogens into the 5-position of the indane moiety resulted in a slight increase in potency for the fluoro compounds **5a,b**, while the chloro and bromo derivatives **7a,b** and **9a,b** showed a reduction in activity in this order. While introduction of a methoxy group in 5-position did not change potency (**11a,b**), larger substituents such as ethoxy diminished inhibitory activity

(**19a,b**) or resulted in a loss of potency as shown for the benzyloxy compound **20a**. The shift of substituents from the 5- into the 6-position of the indane skeleton reduced activity, resulting in moderate or poor inhibitors (**15a**, **21a**, **21b**). A methoxy substituent in position 7 (**26a**) did not affect potency significantly compared to the unsubstituted compound (**1a**). The 4-substituted inhibitors showed very high activity in the case of the fluorinated *E*-isomer and the chloro compounds (**24a**, **25a**, **25b**), while the methylated compounds and the fluorinated *Z*-isomer displayed moderate inhibition (**23a**, **23b**, **24b**).

The most active compounds were tested in V79 MZh cells expressing either CYP11B1 or CYP11B2, respectively, as described recently to get information about activity and selectivity in mammalian cells.^{7,27,28} The same substrate and similar conditions for incubation, extraction, and analysis were used as described for the yeast assay.

Table 2. (4-Pyridylmethylene)tetrahydronaphthalenes and -indanes: Inhibition of Human Adrenal CYP11B1 and CYP11B2, Human CYP17, and Human CYP19 in Vitro

compd	X	isomer	% inhibition		IC ₅₀ (nM)			selectivity factor ^j
			human hCYP11B2 ^{a,b}	human CYP17 ^{c,d}	V79 11B1 hCYP11B1 ^{e,f}	V79 11B2 hCYP11B2 ^{e,g}	human CYP19 ^{h,i}	
2a	H	<i>E</i>	55	nd	nd	8	6700	—
2b	H	<i>Z</i>	nd	1315	931	18	12730	1.4
4a	H	<i>E</i>	54	282	143	15	650	2.0
6a	5-F	<i>E</i>	37	380	1098	15	1550	0.3
6b	5-F	<i>Z</i>	77	257	34	29	800	7.6
8a	5-Cl	<i>E</i>	38	243	1515	18	5430	0.2
8b	5-Cl	<i>Z</i>	37	1122	301	36	1990	3.7
10a	5-Br	<i>E</i>	17	948	2640	24	>36000	0.4
10b	5-Br	<i>Z</i>	40	877	484	56	3400	1.8
12a	5-OMe	<i>E</i>	11	nd	nd	59	3960	—
12b	5-OMe	<i>Z</i>	13	nd	nd	55	3720	—
14a	6-OMe	<i>E</i>	31	nd	nd	22	800	—
14b	6-OMe	<i>Z</i>	36	nd	nd	56	1010	—
16a	6-OMe	<i>E</i>	26	nd	nd	3	280	—
16b	6-OMe	<i>Z</i>	24	nd	nd	26	770	—
18a	6,7-di-OMe	<i>E</i>	29	nd	nd	11	90	—
22a	6-Me	<i>E</i>	41	nd	nd	4	1280	—
22b	6-Me	<i>Z</i>	46	nd	nd	8	1710	—
ketoconazole	—	—	36	224	81	40	nd	2.8
fadrozole	—	—	68	10	1	5	30	10

^a Mean value of four determinations, standard deviation less than 10%. ^b *S. pombe* expressing human CYP11B2; substrate deoxycorticosterone, 100 nM; inhibitor, 500 nM. ^c Mean value of four determinations, standard deviation less than 10%. ^d *E. coli* expressing human CYP17; 5 mg/mL of protein; substrate progesterone, 2.5 μM; inhibitor, 2.5 μM. ^e Mean value of four determinations, standard deviation less than 20%. nd = not determined. ^f Hamster fibroblasts expressing human CYP11B1; substrate deoxycorticosterone, 100 nM. ^g Hamster fibroblasts expressing human CYP11B2; substrate deoxycorticosterone, 100 nM. ^h Mean value of four determinations, standard deviation less than 5%. nd = not determined. ⁱ Human placental CYP19; 1 mg/mL of protein; substrate androstenedione, 500 nM. ^j IC₅₀ CYP11B1/IC₅₀ CYP11B2.

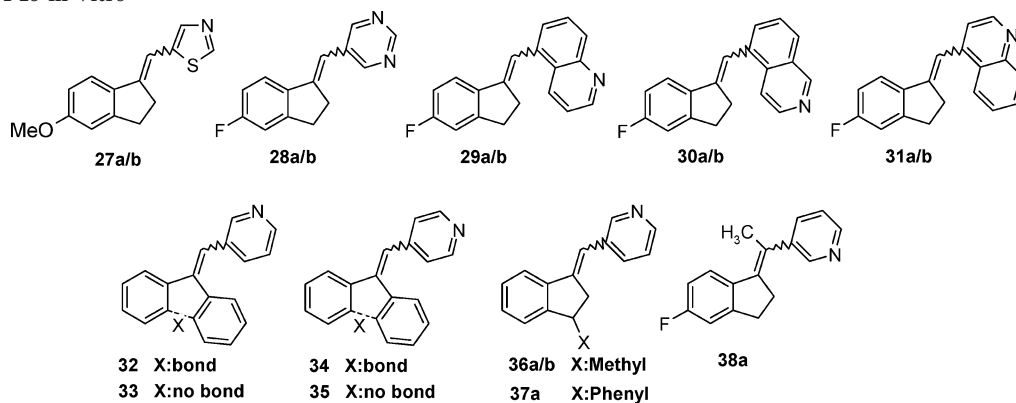
The inhibitors displayed high activities with IC₅₀ values in the range from 7 to 248 nM, except for compound **13b** displaying an IC₅₀ of 878 nM. In most cases, compounds with a high potency—showing IC₅₀ values <30 nM—were *E*-configured indane derivatives (**1a**, **3a**, **5a**, **5b**, **7a**, **11b**, **24a**, **25a**). Additionally, they were highly selective by exhibiting only moderate inhibition of CYP11B1 (IC₅₀ = 86–2700 nM). The only exception was the methoxy-substituted tetraline **13b**, which turned out to be a stronger inhibitor of CYP11B1 with a selectivity factor of 0.2. The unsubstituted derivative **1b** displayed similar inhibition values for both enzymes. The most selective compounds, **1a**, **7a**, and **9a**, were over 50-fold more selective for CYP11B2 in contrast to the reference fadrozole, which displayed (only) a selectivity factor of 10. Comparing the inhibition data for CYP11B2, it was obvious that the *E*-isomers showed a higher potency than the corresponding *Z*-isomers, as had been observed in the yeast system. Especially for compounds **1a,b** and **13a,b** this finding was striking.

The data of the 4-pyridyl-substituted compounds are presented in Table 2. Most of the compounds were only moderate inhibitors of CYP11B2 in the yeast assay. Only one compound out of 18 showed more than 70% inhibition at 500 nM (**6b**). Interestingly, in this class of compounds the *Z*-isomers were more active or showed at least similar potency as the corresponding *E*-isomers.

Regarding the IC₅₀ values obtained with CYP11B2 expressed in V79MZh cells, the data were in good

accordance with the values of the yeast system. Compounds showing moderate percent inhibition values in the yeast system also exhibited low potency in V79 CYP11B2 cells. The IC₅₀ values for CYP11B1 were found to be in a similar range (IC₅₀ CYP11B1 = 243–1315 nM, IC₅₀ CYP11B2 = 34–2640 nM). Compounds **6a**, **8a**, and **10a** turned out to be rather selective for CYP11B1, and the unsubstituted indane **2b** showed similar inhibition values for both enzymes, whereas the other compounds inhibited CYP11B2 stronger than CYP11B1 (**4a**, **6b**, **8b**, **10b**). In contrast to the 3-pyridyl derivatives (Table 1), the 4-pyridyl compounds (Table 2) showed only small differences in selectivity factors between CYP11B2 and CYP11B1. The most active and selective compound in this series was the fluorinated indane **6b** with a 7-fold selectivity for CYP11B2.

Modifications of the skeleton and the heterocycle were performed to explore the available space in the active site of the enzyme (Table 3). While methyl substituents in position three at the indane moiety reduced potency (**36a,b**), the introduction of a phenyl group at C3 as well as the anellation of an additional benzene nucleus at C2/C3 resulted in inactive compounds (**37a**, **32–35**). Introduction of a methyl substituent at the double bond (**38a**) diminished activity and selectivity. The replacement of the pyridyl group by other heterocycles reduced potency in case of the thiazole compound (**27a,b**). A loss in activity was caused by the quinoline-substituted compounds (**29a**, **29b**, **31a**, **31b**). The isoquinoline-substituted *Z*-isomer **30b** and the pyrimidyl-substituted

Table 3. Structural Modifications of the Title Compounds: Inhibition of Human Adrenal CYP11B1 and CYP11B2, Human CYP17, and Human CYP19 in Vitro

compd	isomer	% inhibition		IC ₅₀ (nM)			selectivity factor ^j
		human hCYP11B2 ^{a,b}	human CYP17 ^{c,d}	V79 11B1 hCYP11B1 ^{e,f}	V79 11B2 hCYP11B2 ^{e,g}	human CYP19 ^{h,i}	
27a	<i>E</i>	18	nd	nd	17	4330	—
27b	<i>Z</i>	17	nd	nd	5	4830	—
28a	<i>E</i>	72	3179	27	6	7450	118
28b	<i>Z</i>	14	nd	nd	0	790	—
29a	<i>E</i>	0	nd	nd	14	>36000	—
29b	<i>Z</i>	0	nd	nd	31	>36000	—
30a	<i>E</i>	60	1129	58	57	720	19.5
30b	<i>Z</i>	91	374	26	65	1940	14.4
31a	<i>E</i>	0	nd	nd	20	>36000	—
31b	<i>Z</i>	0	nd	nd	14	>36000	—
32		0	nd	nd	6	4810	—
33		5	nd	nd	9	3630	—
34		6	nd	nd	5	2740	—
35		32	nd	nd	22	100	—
36a	<i>E</i>	47	nd	nd	13	3680	—
36b	<i>Z</i>	15	nd	nd	41	2800	—
37a	<i>E</i>	0	nd	nd	3	4060	—
38a	<i>E</i>	67	159	96	nd	nd	1.7
ketoconazole	—	36	224	81	40	nd	2.8
fadrozole	—	68	10	1	5	30	10

^a Mean value of four determinations, standard deviation less than 10%. ^b *S. pombe* expressing human CYP11B2; substrate deoxycorticosterone, 100 nM; inhibitor, 500 nM. ^c Mean value of four determinations, standard deviation less than 10%. ^d *E. coli* expressing human CYP17; 5 mg/mL of protein; substrate progesterone, 2.5 μM; inhibitor, 2.5 μM. ^e Mean value of four determinations, standard deviation less than 20%. nd = not determined. ^f Hamster fibroblasts expressing human CYP11B1; substrate deoxycorticosterone, 100 nM. ^g Hamster fibroblasts expressing human CYP11B2; substrate deoxycorticosterone, 100 nM. ^h Mean value of four determinations, standard deviation less than 5%. nd = not determined. ⁱ Human placental CYP19; 1 mg/mL of protein; substrate androstenedione, 500 nM. ^j IC₅₀ CYP11B1/IC₅₀ CYP11B2.

E-isomer **28a** turned out to be very potent inhibitors (IC₅₀ < 30 nM) with a 14-fold selectivity for CYP11B2 in case of compound **30b** and a selectivity factor of approximately 120 in case of compound **28a**.

Inhibition of Human CYP19 and CYP17 in Vitro (Tables 1–3). Selectivity of the compounds was also determined for other steroidogenic CYP enzymes: the estrogens producing CYP19 and the androgens forming CYP17. IC₅₀ values of the compounds for CYP19 were determined in vitro using human placental microsomes and [1β-³H]androstenedione as substrate as described by Thompson and Siiteri²⁹ using our modification.³⁰ Only a few compounds exhibited an IC₅₀ value below 200 nM (**18a**, **24b**, **25a**, **35**). As expected, they were less active than the reference compound fadrozole (IC₅₀ = 30 nM). The 6,7-disubstituted methoxy derivative **18a** was the strongest inhibitor in this series, with an IC₅₀ value of 90 nM. Compounds that showed high selectivity factors for CYP11B1 were weak inhibitors of CYP19 (IC₅₀ > 2 μM) (**1a**, **7a**, **9a**, **28a**).

The percent inhibition values of the compounds toward CYP 17 were determined in vitro as described

previously³¹ using progesterone as substrate and the 50 000g sediment of *Escherichia coli* recombinantly expressing human CYP17. Most of the compounds showed weak inhibition at a concentration of 2.5 μM as compared to the reference ketoconazole (40%), and some of them displayed similar activity (**10b**, **11b**, **12a**, **12b**, **14b**, **24a**, **30a**, **30b**, **36b**). Again, the most selective inhibitors toward CYP11B1 (**1a**, **7a**, **9a**, **28a**) showed almost no inhibition of CYP17.

Computational Results

To explain the experimental results, conformational analyses with selected compounds, protein modeling of CYP11B2 and CYP11B1, and docking experiments with chosen compounds were performed.

Conformational Analyses. The halogenated compounds displayed a particularly interesting structure–activity relationship, and it was therefore decided to study their electrostatic and conformational properties in more detail. The fluoro analogues (**5a,b** and **6a,b**) were chosen for exemplary ab initio calculations. Compounds **5a** and **5b** can adopt two conformations, which

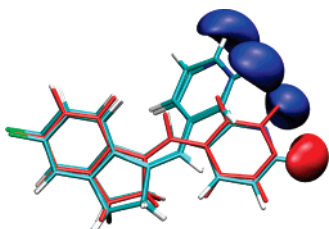


Figure 1. Electrostatic potential isosurfaces of compounds **5a,b** and **6a,b** (-0.05 kcal/mol interaction energy for a $+1$ charge). Compound **6a** and the corresponding isosurface are shown in red, and the other compounds are shown in CPK colors with blue isosurfaces.

differ by the orientation of the pyridine nitrogen. Both conformers were built and their geometries were optimized in order to determine the preferred conformation. The single-point MP2/cc-pVTZ energies of the two conformers of the *E*-isomer **5a** and the *Z*-isomer **5b** differed by only 2.06 and 0.17 kcal/mol, respectively. We therefore assume that either one of the two conformers can bind to the enzyme active site. Graphical representations of the minimum energy conformations of compounds **5a,b** and **6a,b** are given in Figure 1 along with their negative electrostatic potential isosurfaces. Figure 2 shows the negative electrostatic potential of compounds **5a** and **6a** mapped on the solvent-accessible surface.

Protein Modeling and Docking. As there are no experimental structures available for CYP11B2, we recently built a 3D model¹² using the X-ray structure of human CYP2C9³² as template. In the present study, a CYP11B1 model was built in addition using the same strategy. Molecular docking calculations were performed for various inhibitors of Tables 1–3. During the docking process the structural models for the active sites of CYP11B2 and CYP11B1 were further refined through energy minimizations and simulated annealing simulations. The best results (scores) were obtained with the 3-pyridyl compounds **5a,b** and **7a,b**. From these studies it becomes apparent that the I-helix is essential for the binding of the compounds. These findings are confirmed by experimental-site directed mutagenesis—results, indicating that the I-helix of CYP11B2 and CYP11B1 is important for substrate binding.^{33,34}

One major aim of this study was to explain the differences in binding affinity (inhibitory potency) between the 3-pyridyl and the 4-pyridyl compounds. For this purpose, the protein–inhibitor interactions of the 3-pyridyl compounds **7a,b** were compared with those of the 4-pyridyl derivatives **8a,b**. The poses for the best docked complexes (lowest energy score) are given in Figure 3. An important interaction between the protein and the inhibitor is the coordinative bond between the pyridyl nitrogen and the heme iron. For an optimal orbital overlap, the pyridyl moiety should be located perpendicular to the heme group with a straight line from Fe to N to the carbon atom, which is located opposite to the nitrogen in the pyridyl ring. Every distortion from this geometry weakens the interaction. It can be seen from Figure 3 that compounds **7a** and **7b** are very close to this optimum, showing a distortion angle of less than 20° . The chlorinated indane derivative **8b** shows an angle between 20° and 25° , and the corresponding *E*-isomer **8a** one between 25° and 30° . In

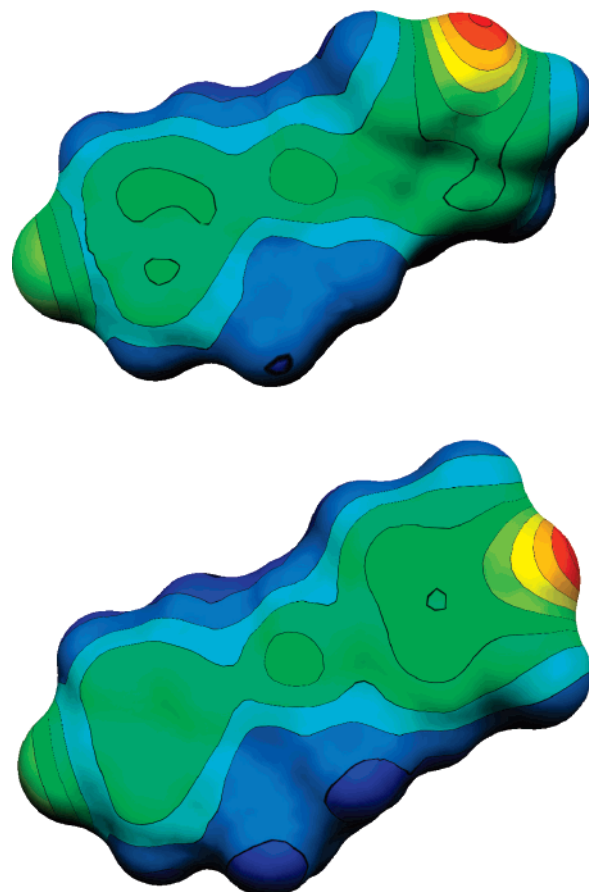


Figure 2. Electrostatic potential (interaction energy for a $+1$ charge in kcal/mol) on the solvent-accessible surface of **5a** and **6a**, color-coded from -0.1 (red) to 0.05 (blue). Compound **5a** is shown at the top and compound **6a** is shown at the bottom.

addition, the pyridyl ring of **8a** is shifted with respect to the heme iron (Figure 3f), thus making the Fe–N coordination almost impossible. The corresponding interaction scores were **7a** = -47.8 kJ/mol, **7b** = -47.7 kJ/mol, **8a** = -12.2 kJ/mol, and **8b** = -30.1 kJ/mol, and they correlated well with the IC_{50} values: **7a** = 26 nM, **7b** = 73 nM, **8a** = 1515 nM, and **8b** = 301 nM. Thus, the position of the pyridyl nitrogen with respect to the heme group is very important for the binding affinity.

In Figure 4 the best poses for compound **28a** docked into the active sites of CYP11B1 and CYP11B2 are presented. As seen for the interaction of the 4-pyridyl compounds with CYP11B2, a larger distortion angle for **28a** bound to CYP11B1 was observed as compared to CYP11B2, explaining the high selectivity of this compound for CYP11B2.

Discussion and Conclusion

The use of CYP11B2 inhibitors as drugs in the therapy of certain cardiovascular diseases is complicated by the need for selectivity to avoid side effects. In the case of the aldosterone receptor antagonist spironolactone, progestational and antiandrogenic effects were observed because of poor selectivity toward the aldosterone receptor.^{4–6} Another unwanted effect of antiminerlocorticoids is hyperkalemia.⁵ Until now, only a few compounds were known to suppress aldosterone formation. Fadrozole, for example, reduced the aldo-

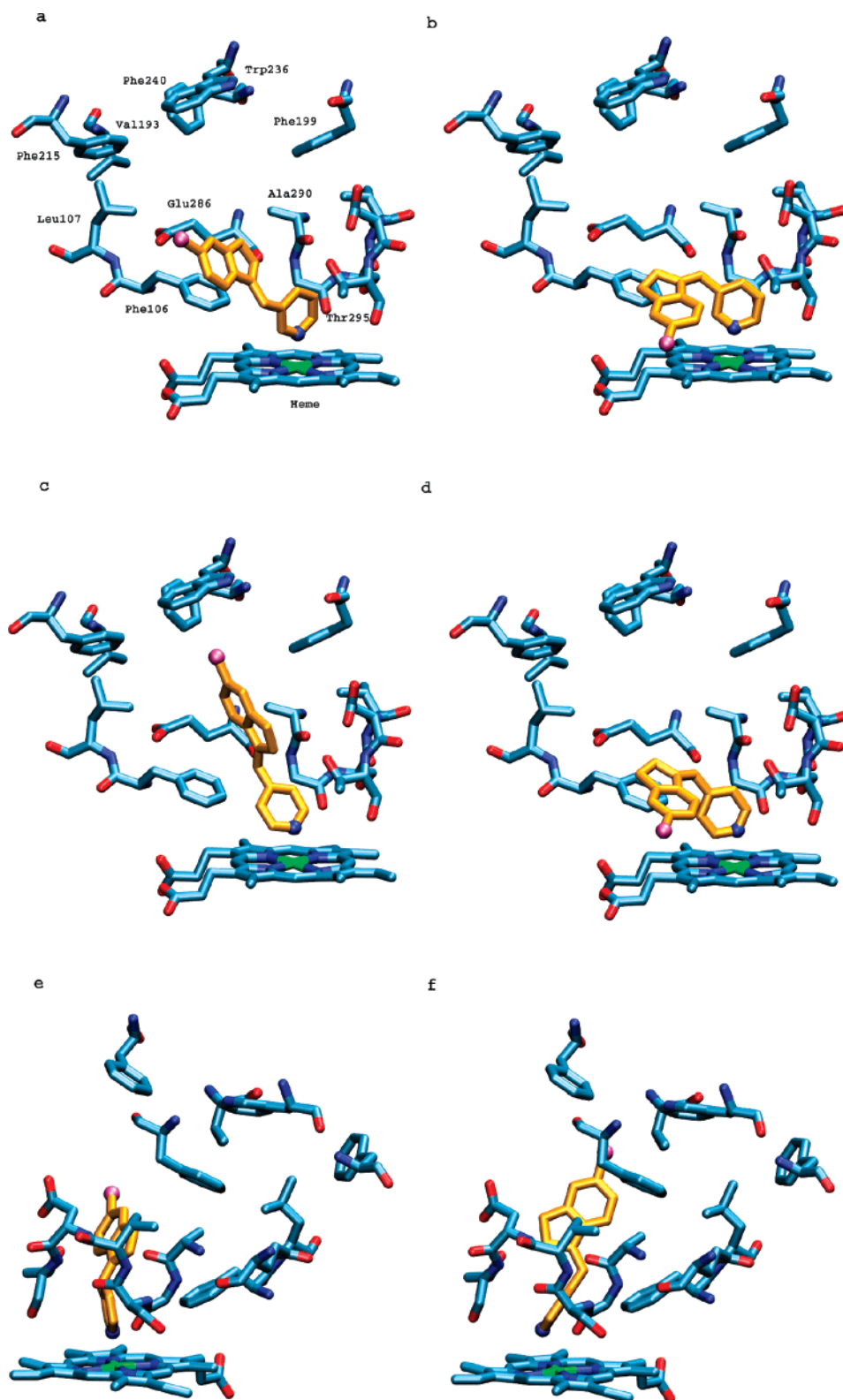


Figure 3. Structure of the CYP11B2–inhibitor complexes (docking result with the lowest energy score). (a and e) **7a** front and side view; (b) **7b**; (c and f) **8a** front and side view; (d) **8b**. The nitrogen atom is blue and the chlorine atom is pink.

sterone and cortisol levels *in vitro*^{35,36} and *in vivo*.¹⁴ Ketoconazole¹⁵ and (imidazolylmethylene)tetrahydronaphthalenes and -indanes¹² displayed moderate¹⁵ or strong¹² inhibitory activity for CYP11B2. However, these compounds showed little or no selectivity toward other CYP enzymes, e.g. CYP11B1, which has a very high sequence homology compared to the target enzyme.^{1,10} Additionally, fadrozole is used as a drug to

reduce estrogen levels in patients with breast cancer.^{13,14} Ketoconazole was shown to reduce androgen levels in disseminated prostatic cancer.³⁷ It is therefore obvious that these inhibitors cannot be used for the treatment of congestive heart failure or myocardial fibrosis. Aiming at the discovery of highly active and more selective inhibitors of CYP11B2, we systematically modified lead compound **III**¹² (Chart 1) in this study.

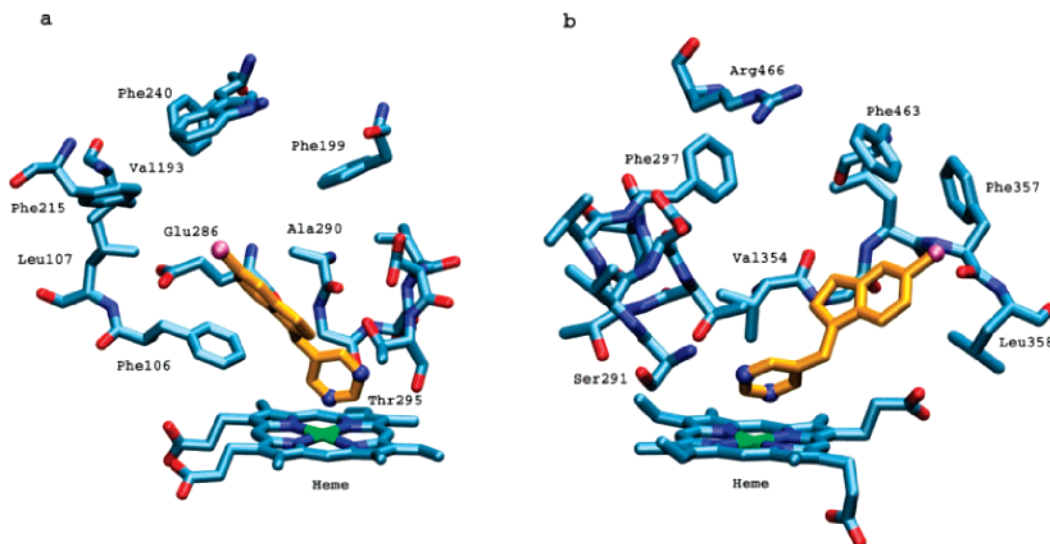


Figure 4. Structure of the CYP11B2–**28a** and CYP11B1–**28a** complexes (docking result with the lowest energy score). The nitrogen atom is blue and the fluorine atom is pink.

Very interesting structure–activity relationships could be observed. The structural requirements, particularly the size of the inhibitor, could be explored: while substitution in the 3- or 6-position at the indane skeleton diminished activity, small groups in the 4-, 5-, or 7-position are appropriate to enhance activity and selectivity of the inhibitors. For complexing the heme iron, the 3-pyridyl moiety was ideal with respect to activity and selectivity. Replacement of the 3-pyridyl group by other nitrogen-containing heterocycles caused a loss in activity and/or selectivity in most cases. The introduction of a pyrimidyl group, however, improved the selectivity of the compounds. In general, most of the compounds described in this study showed a selectivity profile that was much better than that of the parent (imidazolylmethylene)tetrahydronaphthalenes and -indanes. The most selective imidazolyl derivative was 4-fold more active in CYP11B2 than in CYP11B1,¹² whereas the best 3-pyridyl compounds presented in this paper showed more than a 50-fold stronger inhibition of CYP11B2 compared to CYP11B1 (**1a**, **7a**, **9a**). In case of the pyrimidyl compound **28a**, a 118-fold stronger inhibition was observed. It is important to note that the compounds did—unlike fadrozole—not affect the sex hormone synthesizing CYP enzymes CYP17 and CYP19. A few derivatives turned out to inhibit CYP11B1 and CYP11B2 with similar potency (**1b**, **2b**) or showed some selectivity toward CYP11B1 (**6a**, **8a**, **10a**, **13b**).

The examination of the influence of the conformational and electronic properties of a selected subset of compounds on their affinity for CYP11B2 led to interesting results. The *E*- and *Z*-configured, halogenated 3- and 4-pyridyl derivatives (**5a,b**–**10a,b**) showed a remarkable selectivity and affinity profile. This was particularly striking for the fluoro analogues **5a,b** and **6a,b**: These compounds differ by the geometry of the exocyclic double bond and by the position of the pyridine nitrogen. Compound **6a** is special in that it was by about 2 orders of magnitude less potent in the CYP11B2 assay than its analogues, which had a very high affinity for CYP11B2. Compound **6a** is also special since its conformational flexibility does not have an influence on its steric and electronic properties. The only carbon–carbon

bond that has a rotational degree of freedom is the one between the pyridine ring and the exocyclic methylene carbon. A rotation around this bond, however, does not lead to a conformation with a distinct spatial property distribution, as the pyridine nitrogen remains in the same position. These structure–activity properties let us consider compound **6a** as an antitype that could be used to highlight geometrical differences and similarities as compared to its isomers. Figure 2 shows the electrostatic potential on the solvent-accessible surface of **5a** and **6a**, the most active and the least active fluoro compound. It is immediately evident that the shape of the molecules is elongated and very similar. Both compounds contain a region in which the nitrogen lone pair of the pyridine ring causes a negative potential. However, this region is in an axial position for compound **6a** and in an off-axial position for compound **5a**. It is this difference in the electrostatic potential distribution that must be held responsible for the distinct binding behavior of the two compounds.

Minimum-energy conformers of all four fluoro analogues are shown in Figure 1 along with their respective negative electrostatic potential isosurfaces. Compound **6a** and the corresponding isosurface is colored red. This figure shows that the lone pair of the pyridine nitrogen, which coordinates to the heme iron, is in an off-axial position for all highly active compounds (**5a**, **5b**, **6b**). Furthermore, the relative position of the lone pair is rather similar for all highly active compounds, irrespective of the configuration of the exocyclic double bond. A similar structure–activity profile can be seen for all other halogenated compounds. The 4-pyridyl *E*-isomers have the lowest affinity toward CYP11B2.

The discussed experimental and quantum chemical results suggest the following relationship between conformation and activity: In the case of the 3-pyridyl-substituted compounds, the *E*-isomers more strongly inhibit CYP11B2 than the *Z*-isomers. For the recently described imidazolyl as well as for the 4-pyridyl compounds of this paper it is the other way round. In general, the activities of the 4-pyridyl compounds are markedly diminished compared to the 3-pyridyl com-

pounds. All strong inhibitors have bend interaction geometries.

For the explanation of their binding affinities the obtained interaction geometries of the different inhibitors were studied. A closer look at the compounds **7a,b** and **8a,b** (Figure 3) revealed that the angle of the C–N(pyridyl)–Fe straight line formed with the heme plane corresponds with the inhibitory potencies. An angle close to 90° leads to an optimal interaction with the heme iron. The larger the deviation from this geometry, the weaker the inhibition.

To explain the differences in inhibition of the *E*-isomers of 3-pyridyl and 4-pyridyl compounds, it is appropriate to look at the angle between their molecular axis and the plane of the heme group (Figure 3a–d). This angle is approximately 45° for the 3-pyridyl and approximately 90° for the 4-pyridyl derivatives. This observation is in agreement with the geometries observed in the quantum chemical calculations. Due to the small angle, which is formed by the *E*-isomers of the 3-pyridyl compounds, the corresponding compounds fit very well into the L-shaped binding pocket and are optimally bound in a relaxed conformation (Figure 3a,e). In contrary, the *E*-isomers of the 4-pyridyl derivatives collide with the top of the binding pocket opposite to the heme group and are thus distorted, turned to the side, and not able to form a strong Fe–N interaction (Figure 3c,f). The differences in the binding modes of the two *Z*-isomers are much smaller (Figure 3b,d); however, in both cases small distortions are observed. Thus, in the case of the 3-pyridyl derivatives, the *E*-isomers show the highest inhibitory potencies.

For the 4-pyridyl compounds the *Z*-isomers are stronger inhibitors. In contrast to the interaction geometry of the 3-pyridyl compounds showing docking poses which are complementary to the L-shape of the binding pocket of the enzyme, the 4-pyridyl derivatives do not optimally bind. Comparing these results to our former study in which imidazole was introduced instead of 3- or 4-pyridine into the same skeletons,¹² the imidazole series showed similar properties to the 4-pyridyl series, also favoring the *Z*-isomers.

Similar observations are made for the highly active and selective compound **28a**. Docking into the homology models of CYP11B2 and CYP11B1 (Figure 4) revealed that in the case of CYP11B1 the angle between the pyrimidyl moiety and the heme plane is distorted by approximately 30°, leading to a weaker N–Fe interaction compared to the CYP11B2 complex.

Summarizing, it can be concluded that highly active and selective inhibitors of CYP11B2 have been developed by structural variations of the lead compound **III**. The most potent compounds hardly affected other steroidogenic enzymes. The pyrimidyl derivative **28a** turned out to be very active and the most selective inhibitor. This compound and its congeners can be expected to lower the aldosterone level in vivo and to produce little or no side effects by inhibition of other CYP enzymes. If in vivo experiments confirm this hypothesis, the compounds presented in this paper offer a new therapeutic option for the treatment of myocardial fibrosis and congestive heart failure.

Experimental Section

Chemical Methods. Melting points were measured on a Stuart Scientific melting point apparatus SMP3 and are uncorrected. IR spectra were measured on a Bruker Vector 33 FT-infrared spectrometer as a powder. ¹H NMR spectra were recorded on a Bruker DRX-500 (500 MHz) instrument. Chemical shifts are given in parts per million, and TMS was used as the internal standard for spectra obtained in DMSO-*d*₆ and CDCl₃. The allocation of the protons was made by numbering serially the carbon–hydrogens (see Charts 2 and 3, numbers in italics). All coupling constants (*J*) are given in Hz. Elemental analyses were performed at the Inorganic Chemistry Department, Saarland University and are consistent with theoretical values within ±0.4% unless indicated. Reagents and solvents were used as obtained from commercial suppliers without further purification. Flash column chromatography (FCC) was performed using silica gel 60 (40–63 μm), and reaction progress was determined by TLC analyses on ALUGRAM SIL G/UV₂₅₄ (Macherey-Nagel).

The following compounds were prepared according to previously described procedures: 5-ethoxyindan-1-one,³⁸ 5-(benzyloxy)indan-1-one,²¹ 6-methylindan-1-one,³⁹ 7-methoxyindan-1-one,⁴⁰ 3-(2-fluorophenyl)acrylic acid,^{41,42} 3-(2-fluorophenyl)propanoic acid,⁴³ 3-(2-fluorophenyl)propanoyl chloride,^{43,44} 4-fluoroindan-1-one,⁴³ 3-(2-chlorophenyl)propanoyl chloride,⁴³ 4-chloroindan-1-one,⁴³ 1,3-thiazole-5-carbaldehyde,²⁵ and pyrimidine-5-carbaldehyde.²⁶

Method A. General Procedure for the Synthesis of Compounds 1–38. Ketone (50 mmol) was dissolved in a mixture of methanol (100 mL) and THF (100 mL), and 1.89 g of NaBH₄ (50 mmol) was added in portions while the reaction mixture cooled to 0 °C. After 10 min at 0 °C, the solution was stirred for 1 h at room temperature. The reaction mixture was diluted with water, and the product was extracted with diethyl ether. The organic phase was washed with 1 N HCl, followed by a saturated solution of NaHCO₃ and finally with water. It was dried over MgSO₄ and the solvent was evaporated. For transferring the resulting alcohol into the phosphonium salt, amounts of 40 mmol of the alcohol and 13.7 g of triphenylphosphonium bromide¹⁹ (40 mmol) were suspended in 30 mL of benzene and refluxed for 12 h under a nitrogen atmosphere. The precipitate was filtered off and dried. The solid was suspended in dry diethyl ether and stirred for 10 min. The phosphonium salt was filtered and washed with diethyl ether. A suspension of 5 mmol of phosphonium salt; 5 mmol of either nicotinaldehyde, isonicotinaldehyde, 1,3-thiazole-5-carbaldehyde, pyrimidine-5-carbaldehyde, quinoline-4-carbaldehyde, quinoline-5-carbaldehyde, isoquinoline-4-carbaldehyde, or 1-pyridin-3-ylethanone; 50 mmol of K₂CO₃; and a few milligrams of 18-crown-6 in 25 mL of dry dichloromethane was refluxed for 12 h under nitrogen atmosphere. The reaction mixture was poured into water and extracted several times with dichloromethane. The combined organic phases were dried over MgSO₄ and the solvent was evaporated. After purification, either the free base was dissolved in acetone and an excess of oxalic acid in acetone was added to get the oxalate or it was dissolved in dry diethyl ether and an excess of HCl in diethyl ether was added to get the hydrochloride.

3-1(*E*)-2,3-Dihydro-1*H*-inden-1-ylidenemethyl]pyridine Hydrochloride (1a). Purification: FCC (EtOAc/hexane, 1:1). Yield: 53%, white solid. Mp: 235 °C. ¹H NMR (500 MHz, DMSO-*d*₆): δ 3.10–3.15 (m, 4H, H-2, H-3), 7.20 (s, 1H, H-8), 7.33–7.35 (m, 2H, H-5, H-6), 7.39–7.41 (m, 1H, H-4), 7.76–7.78 (m, 1H, H-7), 7.89–7.92 (m, 1H, H-13), 8.45 (d, ³*J* = 8.2 Hz, 1H, H-14), 8.65 (dd, ³*J* = 5.4 Hz, ⁴*J* = 1.3 Hz, 1H, H-12), 8.90 (s, 1H, H-10). IR cm⁻¹: ν_{max} 2411, 1636, 1551, 1471, 825, 806, 751. Anal. (C₁₅H₁₃N·HCl·0.3H₂O): C, H, N.

3-1(*Z*)-2,3-Dihydro-1*H*-inden-1-ylidenemethyl]pyridine Hydrochloride (1b). Purification: FCC (EtOAc/hexane, 1:1). Yield: 22%, white solid. Mp: 229 °C. ¹H NMR (500 MHz, DMSO-*d*₆): δ 2.91–2.95 (m, 2H, H-2), 2.98–3.01 (m, 2H, H-3), 6.63 (s, 1H, H-8), 7.00–7.06 (m, 2H, H-5, H-6), 7.25–7.40 (m, 2H, H-4, H-7), 7.88 (dd, ³*J* = 5.5 Hz, ³*J* = 8.0 Hz, 1H, H-13), 8.34 (d, ³*J* = 7.4 Hz, 1H, H-14), 8.73 (d, ³*J* = 5.4 Hz, 1H, H-12),

8.81 (s, 1H, H-10). IR cm^{-1} : ν_{max} 3022, 2934, 2841, 2427, 1609, 1548, 1455, 1016, 902, 815, 760, 749. Anal. ($\text{C}_{15}\text{H}_{13}\text{N}\cdot\text{HCl}$): C, H, N.

4-[(E)-2,3-Dihydro-1H-inden-1-ylidenemethyl]pyridine Oxalate (2a). Purification: FCC (acetone/petrol ether, 3:10). Yield: 33%, yellow solid. Mp: 167 °C. ^1H NMR (400 MHz, $\text{DMSO}-d_6$): δ 3.10–3.15 (m, 4H, H-2, H-3), 7.10 (s, 1H, H-8), 7.29–7.40 (m, 3H, H-4, H-5, H-6), 7.55 (d, $^3J = 6.1$ Hz, 2H, H-10, H-14), 7.78–7.80 (m, 1H, H-7), 8.59 (d, $^3J = 6.1$ Hz, 2H, H-11, H-13). IR (KBr) cm^{-1} : ν_{max} 1660, 1610, 1510, 900, 830, 810, 760, 750, 730, 710. Anal. ($\text{C}_{15}\text{H}_{13}\text{N}\cdot\text{C}_2\text{H}_2\text{O}_4$): C, H, N.

4-[(Z)-2,3-Dihydro-1H-inden-1-ylidenemethyl]pyridine Oxalate (2b). Purification: FCC (acetone/petrol ether, 3:10). Yield: 22%, pale yellow solid. Mp: 140 °C. ^1H NMR (400 MHz, $\text{DMSO}-d_6$): δ 2.88–2.91 (m, 2H, H-2), 2.95–2.99 (m, 2H, H-3), 6.58 (s, 1H, H-8), 7.03 (t, $^3J = 7.7$ Hz, 1H, H-5), 7.19–7.26 (m, 2H, H-4, H-6), 7.35 (d, $^3J = 7.6$ Hz, 1H, H-7), 7.40 (d, $^3J = 6.0$ Hz, 2H, H-10, H-14), 8.57 (d, $^3J = 6.0$ Hz, 2H, H-11, H-13). IR (KBr) cm^{-1} : ν_{max} 3080, 3040, 1610, 1500, 900, 840, 820, 760, 750, 700. Anal. ($\text{C}_{15}\text{H}_{13}\text{N}\cdot\text{C}_2\text{H}_2\text{O}_4$): C, H, N.

3-[(E)-3,4-Dihydronaphthalen-1(2H)-ylidenemethyl]pyridine Hydrochloride (3a). Purification: FCC (EtOAc/hexane, 1:1). Yield: 46%, white solid. Mp: 209 °C. ^1H NMR (500 MHz, $\text{DMSO}-d_6$): δ 1.76–1.81 (m, 2H, H-3), 2.77–2.83 (m, 4H, H-2, H-4), 7.19–7.29 (m, 4H, H-5, H-6, H-7, H-8), 7.83–7.85 (m, 1H, H-14), 7.97 (s, 1H, H-9), 8.48 (d, $^3J = 8.2$ Hz, 1H, H-15), 8.73 (d, $^3J = 5.7$ Hz, 1H, H-13), 8.90 (s, 1H, H-11). IR cm^{-1} : ν_{max} 3056, 3019, 2953, 2278, 1621, 1569, 1460, 1351, 860, 818, 789, 756. Anal. ($\text{C}_{16}\text{H}_{15}\text{N}\cdot\text{HCl}$): C, H, N.

3-[(Z)-3,4-Dihydronaphthalen-1(2H)-ylidenemethyl]pyridine Hydrochloride (3b). Purification: FCC (EtOAc/hexane, 1:1). Yield: 18%, white solid. Mp: 206 °C. ^1H NMR (500 MHz, $\text{DMSO}-d_6$): δ 1.98 (m, $^3J = 6.6$ Hz, 2H, H-3), 2.55 (t, $^3J = 6.6$ Hz, 2H, H-2), 2.88 (t, $^3J = 6.7$ Hz, 2H, H-4), 6.52 (s, 1H, H-9), 6.88–6.96 (m, 2H, H-6, H-7), 7.18–7.24 (m, 2H, H-5, H-8), 7.74 (d, $^3J = 8.1$ Hz, 1H, H-14), 8.31 (d, $^3J = 8.3$ Hz, 1H, H-15), 8.59–8.62 (m, 2H, H-13, H-11). IR cm^{-1} : ν_{max} 3046, 2936, 1524, 1458, 813, 757. Anal. ($\text{C}_{16}\text{H}_{15}\text{N}\cdot\text{HCl}$): C, H, N.

4-[(E)-3,4-Dihydronaphthalen-1(2H)-ylidenemethyl]pyridine (4a). Purification: crystallization from hexane. Yield: 43%, pale green crystals. Mp: 66 °C. ^1H NMR (400 MHz, $\text{DMSO}-d_6$): δ 1.63–1.69 (m, 2H, H-3), 2.78–2.86 (m, 4H, H-2, H-4), 6.92 (s, 1H, H-9), 7.13–7.15 (m, 1H, H-7), 7.20–7.26 (m, 4H, H-5, H-6, H-11, H-15), 7.68–7.71 (m, 1H, H-8), 8.58 (dd, $^3J = 4.7$ Hz, $^4J = 1.4$ Hz, 2H, H-12, H-14). IR (KBr) cm^{-1} : ν_{max} 3080, 3040, 1610, 1500, 840, 820, 760, 750, 700. Anal. ($\text{C}_{16}\text{H}_{15}\text{N}$): C, H, N.

Biological Methods. 1. Enzyme Preparations. CYP17 and CYP19 were prepared according to described methods: the 50 000g sediment of human CYP17 expressing *E. coli*³¹ and microsomes from human placenta for CYP19.³⁰

2. Enzyme Assays. The following enzyme assays were performed as described: CYP17 assay³¹ and CYP19 assay.³⁰

3. Fission Yeast Assay. Fission yeast expressing human CYP11B2 (*Schizosaccharomyces pombe* PE1) was incubated with [4-¹⁴C]-11-deoxycorticosterone as substrate and inhibitor at a concentration of 500 nM.⁷ The enzyme reaction was stopped by extraction with ethyl acetate. The conversion of the substrate was analyzed by HPTLC and a phosphoimaging system as described.^{7,12}

4. Activity and Selectivity Assay Using V79 Cells. V79 MZh 11B1 and V79 MZh 11B2 cells^{27,28} were incubated with [4-¹⁴C]-11-deoxycorticosterone as substrate and inhibitor in at least three different concentrations. The enzyme reactions were stopped by addition of ethyl acetate. After vigorous shaking and a centrifugation step (10 000g, 2 min) the steroids were extracted into the organic phase, which was then separated. The steroids were analyzed by HPTLC using a phosphoimager as described.^{7,12}

Computational Results. 1. Conformational Analysis. The Gaussian 03 software (Gaussian Inc., Pittsburgh PA, 2003) was used for all calculations. The three-dimensional

structures of compounds **5a,b** and **6a,b** were initially optimized at the BLYP/cc-pVDZ^{45–47} level of theory. For compounds **5a,b**, two alternative conformers that differed by the orientation of the pyridine nitrogen were studied. Single-point MP2/cc-pVTZ^{47,48} calculations were performed on the optimized structures to determine their electronic properties. The results were visualized using the VMD and Molekel programs.^{49,50}

2. Protein Modeling and Docking. Using the recently resolved human cytochrome CYP2C9 structure (PDB code 1OG5)³² as template, homology models were built for CYP11B1 and CYP11B2. For this purpose, first a multiple sequence alignment was performed using a variety of methods through the structure prediction meta-server 3D-Jury.⁵¹ The results were critically compared and the alignment with the sequence of CYP2C9 was found to be the best. On the basis of this alignment, 3D models were created with Swiss-Model,⁵² the WHATIF server,⁵³ and Nest,⁵⁴ using CYP2C9 as the template structure. All side chains were placed using SQWRL3.⁵⁵ The resulting models were critically compared. No significant differences were observed in proximity to the binding pocket. The final models were energy-minimized. Afterward several known inhibitors were docked and the binding pocket geometry was further refined through energy minimization and simulated annealing procedures. All energy minimization/simulated annealing calculations were performed using the GROMACS united atom force field and molecular dynamics program.⁵⁶ For the docking studies the docking program FlexX-Pharm was used.⁵⁷ A pharmacophore constraint was applied to ensure the right binding mode of the inhibitors with the heme cofactor. For this purpose, a directed heme-Fe–N interaction was defined perpendicular to the heme plane. The constraint requires the existence of an inhibitor nitrogen atom on the surface of an interaction cone with a 20° radius that has its origin at the Fe atom and points perpendicular to the heme plane (with a length of 2.2 Å). Only docking solutions were accepted which fulfilled this constraint. From these solutions the inhibitor conformation with the lowest docking score was used for the further analyses of the binding mode and the interactions with the binding pocket. Due to its incremental construction algorithm, the FlexPharm program samples all possible inhibitor conformers at each full docking calculation. During the simulated annealing procedure the protein was cooled from 400 to 0 K over 20 ps. Several temperature ranges (800–0, 600–0, and 400–0 K) were explored during the initial testing and 400 K was found to be sufficiently high for the proposed protocol. A cutoff of 14 Å was used for the nonbonded interactions. The solvent was approximated through a dielectric constant of 4.0. This value was chosen because our interest was focused on the conformational changes inside the binding pocket. Position restraints of 1000 were applied to all backbone atoms and the heme moiety.

Acknowledgment. We thank the Deutsche Forschungsgemeinschaft (Ha 1513/6), the Saarland Ministry of Education (ETTT Project), and the Fonds der Chemischen Industrie for financial support. S.U. is grateful to the Fonds der Chemischen Industrie and the Bundesministerium für Bildung und Forschung for a scholarship (Kekule's grant). U.M.-V. is grateful to Saarland University for a scholarship (Landesgraduierten-Förderung). We thank Ms. Anja Paluszczak and Ms. Martina Palzer for their help in performing the in vitro tests. Thanks are due to Prof. Rita Bernhardt, Saarland University, for supplying us with the V79 cells. The Swiss Supercomputer Center (SCS) kindly provided CPU time for the ab initio calculations.

Supporting Information Available: Analytical and spectroscopic data (NMR, IR) of synthesized compounds **5–38** and table of elemental analysis of compounds **1–38**. This material is available free of charge via the Internet at <http://pubs.acs.org>.

References

- (1) Kawamoto, T.; Mitsuuchi, Y.; Toda, K.; Yokoyama, Y.; Miyahara, K.; Miura, S.; Ohnishi, T.; Ichikawa, Y.; Nakao, K.; Imura, H. Role of steroid 11 beta-hydroxylase and steroid 18-hydroxylase in the biosynthesis of glucocorticoids and mineralocorticoids in humans. *Proc. Natl. Acad. Sci. U.S.A.* **1992**, *89*, 1458–1462.
- (2) Brilla, C. G. Renin-angiotensin-aldosterone system and myocardial fibrosis. *Cardiovasc. Res.* **2000**, *47*, 1–3.
- (3) Pitt, B.; Remme, W.; Zannad, F.; Neaton, J.; Martinez, F.; Roniker, B.; Bittman, R.; Hurley, S.; Kleiman, J.; Gatlin, M. Eplerenone, a selective aldosterone blocker, in patients with left ventricular dysfunction after myocardial infarction. *N. Engl. J. Med.* **2003**, *348*, 1309–1321.
- (4) Pitt, B.; Zannad, F.; Remme, W. J.; Cody, R.; Castaigne, A.; Perez, A.; Palensky, J.; Wittes, J. The effect of spironolactone on morbidity and mortality in patients with severe heart failure. Randomized Aldactone Evaluation Study Investigators. *N. Engl. J. Med.* **1999**, *341*, 709–717.
- (5) Christ, M.; Grimm, W.; Maisch, B. Significance of aldosterone antagonist therapy. *Internist (Berlin)* **2004**, *45*, 347–354.
- (6) Delyani, J. A. Mineralocorticoid receptor antagonists: The evolution of utility and pharmacology. *Kidney Int.* **2000**, *57*, 1408–1411.
- (7) Ehmer, P. B.; Bureik, M.; Bernhardt, R.; Müller, U.; Hartmann, R. W. Development of a test system for inhibitors of human aldosterone synthase (CYP11B2): Screening in fission yeast and evaluation of selectivity in V79 cells. *J. Steroid Biochem. Mol. Biol.* **2002**, *81*, 173–179.
- (8) Hartmann, R. W.; Müller, U.; Ehmer, P. B. Discovery of selective CYP11B2 (aldosterone synthase) inhibitors for the therapy of congestive heart failure and myocardial fibrosis. *Eur. J. Med. Chem.* **2003**, *38*, 363–366.
- (9) Baumann, C. K.; Aebi, S. Aromatase inhibitors in the adjuvant therapy of breast carcinomas. *Ther. Umsch.* **2004**, *61*, 359–364.
- (10) Pilon, C.; Mulatero, P.; Barzon, P.; Veglio, F.; Garrone, C.; Boscaro, M.; Sonino, N.; Fallo, F. Mutations in CYP11B1 gene converting 11beta-hydroxylase into an aldosterone-producing enzyme are not present in aldosterone-producing adenomas. *J. Clin. Endocrinol. Metab.* **1999**, *84*, 4228–4231.
- (11) Wisconsin Package Version 10.1, Genetics Computer Group (GCG), Madison, WI.
- (12) Ulmschneider, S.; Müller-Vieira, U.; Mitrenga, M.; Hartmann, R. W.; Oberwinkler-Marchais, S.; Klein, C. D.; Bureik, M.; Bernhardt, R.; Antes, I.; Lengauer, T. Synthesis and evaluation of imidazolylmethylene-tetrahydronaphthalenes and imidazolylmethylene-indanes: Potent inhibitors of aldosterone synthase. *J. Med. Chem.* **2004**, in press (available online: <http://dx.doi.org/10.1021/jm049600p>).
- (13) Dowsett, M.; Stein, R. C.; Mehta, A.; Coombes, R. C. Potency and selectivity of the nonsteroidal aromatase inhibitor CGS 16949A in postmenopausal breast cancer patients. *Clin. Endocrinol. (Oxford)* **1990**, *32*, 623–634.
- (14) Demers, L. M.; Melby, J. C.; Wilson, T. E.; Lipton, A.; Harvey, H. A.; Santen, R. J. The effects of CGS 16949A, an aromatase inhibitor on adrenal mineralocorticoid biosynthesis. *J. Clin. Endocrinol. Metab.* **1990**, *70*, 1162–1166.
- (15) Bureik, M.; Hubel, K.; Dragan, C. A.; Scher, J.; Becker, H.; Lenz, N.; Bernhardt, R. Development of test systems for the discovery of selective human aldosterone synthase (CYP11B2) and 11beta-hydroxylase (CYP11B1) inhibitors. Discovery of a new lead compound for the therapy of congestive heart failure, myocardial fibrosis and hypertension. *Mol. Cell. Endocrinol.* **2004**, *217*, 249–254.
- (16) Hartmann, R. W. Selective inhibition of steroidogenic P450 enzymes: Current status and future perspectives. *Eur. J. Pharm. Sci.* **1994**, *15*–16.
- (17) Van Wauwe, J. P.; Janssen, P. A. Is there a case for P-450 inhibitors in cancer treatment? *J. Med. Chem.* **1989**, *32*, 2231–2239.
- (18) El Ahmad, Y.; Laurent, E.; Maillet, P.; Talab, A.; Teste, J. F.; Dokhan, R.; Tran, G.; Ollivier, R. New benzocycloalkylpiperazines, potent and selective 5-HT1A receptor ligands. *J. Med. Chem.* **1997**, *40*, 952–960.
- (19) Hercouet, A.; Le Corre, M. Triphenylphosphonium bromide: A convenient and quantitative source of gaseous hydrogen bromide. *Synth. Commun.* **1988**, *157*–158.
- (20) Reimann, E.; Hargasser, E. Synthese von *cis*-9,11a-dimethyl-4,5,6,6a,7a,8,9,10,11,11a-decahydro-7H-naphtho(1,8-fg)isoquinolinen (Synthesis of *cis*-9,11a-dimethyl-4,5,6,6a,7a,8,9,10,11,11a-decahydro-7H-naphtho(1,8-fg)isoquinolines). *Arch. Pharm.* **1989**, *327*, 159–164.
- (21) Donbrow, M. Cyclisation and debenzoylation of m-benzyloxypropionic acid as competitive reactions. *J. Chem. Soc.* **1959**, 1613–1615.
- (22) Budhram, R. S.; Palaniswamy, V. A.; Eisenbraun, E. J. Steric effects in the synthesis of 1,7-dialkylindanes. *J. Org. Chem.* **1986**, *51*, 1402–1406.
- (23) Rabjohn, M. 2,3-Dimethoxycinnamic acid. *Org. Synth. Collect.* **1963**, 327–329.
- (24) Musso, D. L.; Cochran, F. R.; Kelley, J. L.; McLean, E. W.; Selph, J. L.; Rigdon, G. C.; Orr, G. F.; Davis, R. G.; Cooper, B. R.; Styles, V. L.; Thompson, J. B.; Hall, W. R. Indanylidene. 1. Design and synthesis of (E)-2-(4,6-difluoro-1-indanylidene)acetamide, a potent, centrally acting muscle relaxant with antiinflammatory and analgesic activity. *J. Med. Chem.* **2003**, *46*, 399–408.
- (25) Dondoni, A.; Fantin, G.; Fogagnolo, M.; Medici, A.; Pedrini, P. A new convenient preparation of 2-, 4-, and 5-thiazolecarboxaldehydes and their conversion into the corresponding carbonitrile N-oxides: Synthesis of 3-thiazolyl-isoxazoles and 3-thiazolyl-isoxazolines. *Synthesis* **1987**, *11*, 998–1001.
- (26) Rho, T.; Abuh, Y. F. One pot synthesis of pyrimidine-5-carboxaldehyde and ethyl pyrimidine-5-carboxylate by utilizing pyrimidin-5-yl-lithium. *Synth. Commun.* **1994**, *24*, 253–256.
- (27) Denner, K.; Doehmer, J.; Bernhardt, R. Cloning of CYP11B1 and CYP11B2 from normal human adrenal and their functional expression in COS-7 and V79 chinese hamster cells. *Endocr. Res.* **1995**, *21*, 443–448.
- (28) Denner, K.; Vogel, R.; Schmalix, W.; Doehmer, J.; Bernhardt, R. Cloning and stable expression of the human mitochondrial cytochrome P45011B1 cDNA in V79 chinese hamster cells and their application for testing of potential inhibitors. *Pharmacogenetics* **1995**, *5*, 89–96.
- (29) Thompson, E. A., Jr.; Siiteri, P. K. Utilization of oxygen and reduced nicotinamide adenine dinucleotide phosphate by human placental microsomes during aromatization of androstenedione. *J. Biol. Chem.* **1974**, *249*, 5364–5372.
- (30) Hartmann, R. W.; Batzl, C. Aromatase inhibitors. Synthesis and evaluation of mammary tumor inhibiting activity of 3-alkylated 3-(4-aminophenyl)piperidine-2,6-diones. *J. Med. Chem.* **1986**, *29*, 1362–1369.
- (31) Hutschenreuter, T. U.; Ehmer, P. B.; Hartmann, R. W. Synthesis of hydroxy derivatives of highly potent nonsteroidal CYP17 inhibitors as potential metabolites and evaluation of their activity by a non cellular assay using recombinant enzyme. *J. Enzyme Inhib. Med. Chem.* **2004**, *19*, 17–32.
- (32) Williams, P. A.; Cosme, J.; Ward, A.; Angove, H. C.; Matak Vinkovic, D.; Jhoti, H. Crystal structure of human cytochrome P4502C9 with bound warfarin. *Nature* **2003**, *424*, 464–468.
- (33) Böttner, B.; Bernhardt, R. Changed ratios of glucocorticoids/mineralocorticoids caused by point mutations in the putative I-helix regions of CYP11B1 and CYP11B2. *Endocr. Res.* **1996**, *22*, 455–461.
- (34) Böttner, B.; Schrauber, H.; Bernhardt, R. Engineering a mineralocorticoid- to a glucocorticoid-synthesizing cytochrome P450. *J. Biol. Chem.* **1996**, *271*, 8028–8033.
- (35) Häusler, A.; Monnet, G.; Borer, C.; Bhatnagar, A. S. Evidence that corticosterone is not an obligatory intermediate in aldosterone biosynthesis in the rat adrenal. *J. Steroid Biochem.* **1989**, *34*, 567–570.
- (36) Bhatnagar, A. S.; Häusler, A.; Schieweck, K.; Lang, M.; Bowman, R. Highly selective inhibition of estrogen biosynthesis by CGS 20267, a new nonsteroidal aromatase inhibitor. *J. Steroid Biochem. Mol. Biol.* **1990**, *37*, 1021–1027.
- (37) De Coster, R.; Caers, I.; Coene, M. C.; Amery, W.; Beerens, D.; Haelterman, C. Effects of high dose ketoconazole therapy on the main plasma testicular and adrenal steroids in previously untreated prostatic cancer patients. *Clin. Endocrinol. (Oxford)* **1986**, *24*, 657–664.
- (38) Albrecht, R.; Schröder, E. Chemotherapeutic nitro-heterocyclic compounds. 3. Preparation of nitrofurfurylidene-, nitrothienylidene- and nitropyrrrolylmethylene-derivatives of substituted 1-indanones and 1.2.3.4-tetrahydro-1-naphthalenones. *Justus Liebig's Ann. Chem.* **1970**, *736*, 110–125.
- (39) Horwell, D. C.; Howson, W.; Nolan, W. P.; S., R. G.; Rees, D. C.; Willems, H. M. G. The design of dipeptidic helical mimetics, part I: The synthesis of 1,6-disubstituted indanes. *Tetrahedron* **1995**, *51*, 203–216.
- (40) Takeuchi, R.; Yasue, H. Rhodium complex-catalyzed desilylative cyclocarbonylation of 1-aryl-2-(trimethylsilyl)acetylenes: A new route to 2,3-dihydro-1H-inden-1-ones. *J. Org. Chem.* **1993**, *58*, 5386–5392.
- (41) Luo, J.-K.; Castle, S. L.; Castle, R. N. The synthesis of difluoro-(1) benzothieno<2,3-c>quinolines and their N-methyl quaternary salts. *J. Heterocycl. Chem.* **1990**, *27*, 2047–2052.
- (42) Yuzikhin, O. S.; Vasil'ev, A. V.; Rudenko, A. P. Oxidation of aromatic compounds: VIII. Oxidative dehydrodimerization of cinnamic acid derivatives in the system CF₃COOH–CH₂Cl₂–PbO₂. *Russ. J. Org. Chem.* **2000**, *36*, 1743–1754.
- (43) Olivier, M.; Marechal, E. Etude de monomeres halogenes et de leur polymerisation cationique. I.- Synthese de divers fluoroindenes (Study on halogenated monomers and their cationic polymerisation. Synthesis of several fluoro-indenes). *Bull. Soc. Chim. Fr.* **1973**, 3092–3095.

- (44) Houghton, R. P.; Voyle, M.; Price, R. Reactions of coordinated ligands. Part 10. Rhodium-catalysed cyclisation of 3-(2-fluorophenyl)propanols to chromans. *J. Chem. Soc., Perkin. Trans. 1* **1984**, *5*, 925–931.
- (45) Becke, A. D. Density-functional exchange-energy approximation with the correct asymptotic behaviour. *Phys. Rev. A* **1988**, *38*, 3098–3100.
- (46) Lee, C. L.; Yang, W.; Parr, R. G. Development of the Colle-Salvetti correlation-energy formula into a functional of the electron density. *Phys. Rev. B* **1988**, *37*, 785–789.
- (47) Dunning, T. H., Jr. Gaussian basis sets for use in correlated molecular calculations. I. The atoms boron through neon and hydrogen. *J. Chem. Phys.* **1989**, *90*, 1007–1023.
- (48) Moller, C.; Plesset, M. S. Note on an approximation treatment for many-electron systems. *Phys. Rev.* **1934**, *46*, 618.
- (49) Flükiger, P.; Lüthi, H. P.; Portmann, S.; Weber, J. MOLEKEL 4.0, Swiss Center for Scientific Computing, Manno (Switzerland), 2000.
- (50) Humphrey, W.; Dalke, A.; Schulten, K. VMD—Visual Molecular Dynamics. *J. Mol. Graph.* **1996**, *14*, 33–38.
- (51) Ginalski, K.; Elofsson, A.; Fischer, D.; Rychlewski, L. 3D-Jury: A simple approach to improve protein structure predictions. *Bioinformatics* **2003**, *19*, 1015–1018.
- (52) Schwede, T.; Kopp, J.; Guex, N.; Peitsch, M. C. SWISS-MODEL: An automated protein homology-modeling server. *Nucleic Acids Res.* **2003**, *31*, 3381–3385.
- (53) Rodriguez, R.; Chinea, G.; Lopez, N.; Pons, T.; Vriend, G. Homology modeling, model and software evaluation: Three related resources. *Bioinformatics* **1998**, *14*, 523–528.
- (54) Petrey, D.; Xiang, Z.; Tang, C. L.; Xie, L.; Gimpelev, M.; Mitros, T.; Soto, C. S.; Goldsmith-Fischman, S.; Kernysky, A.; Schlessinger, A.; Koh, I. Y.; Alexov, E.; Honig, B. Using multiple structure alignments, fast model building, and energetic analysis in fold recognition and homology modeling. *Proteins* **2003**, *53 Suppl 6*, 430–435.
- (55) Canutescu, A. A.; Shelenkov, A. A.; Dunbrack, R. L., Jr. A graph-theory algorithm for rapid protein side-chain prediction. *Protein Sci.* **2003**, *12*, 2001–2014.
- (56) Lindahl, E.; Hess, B.; van der Spoel, D. GROMACS 3.0: A package for molecular simulation and trajectory analysis. *J. Mol. Mod.* **2001**, *7*, 306–317.
- (57) Hindle, S. A.; Rarey, M.; Buning, C.; Lengauer, T. Flexible docking under pharmacophore type constraints. *J. Comput. Aid. Mol. Des.* **2002**, *16*, 129–149.

JM0492397